Journal of
Micro/Nanolithography, MEMS, and MOEMS

SPIEDigitalLibrary.org/jm3

Microelectromechanical torsional varactors with low parasitic capacitances and high dynamic range

Chenniappan Venkatesh
Navakanta Bhat
K. J. Vinoy
Satish Grandhi

SPIE

Microelectromechanical torsional varactors with low parasitic capacitances and high dynamic range

Chenniappan Venkatesh
Navakanta Bhat
K. J. Vinoy
Satish Grandhi
Indian Institute of Science
Department of Electrical Communication Engineering
Bangalore 560012, India
E-mail: cvenkat_mems@yahoo.co.in

Abstract. This work focuses on the design of torsional microelectromechanical systems (MEMS) varactors to achieve highdynamic range of capacitances. MEMS varactors fabricated through the polyMUMPS process are characterized at low and high frequencies for their capacitance-voltage characteristics and electrical parasitics. The effect of parasitic capacitances on tuning ratio is studied and an equivalent circuit is developed. Two variants of torsional varactors that help to improve the dynamic range of torsional varactors despite the parasitics are proposed and characterized. A tuning ratio of 1:8, which is the highest reported in literature, has been obtained. We also demonstrate through simulations that much higher tuning ratios can be obtained with the designs proposed. The designs and experimental results presented are relevant to CMOS fabrication processes that use low resistivity substrate. [DOI: 10.1117/1.JMM.11.1.013006]

Subject terms: MEMS varactors; tuning ratio; parasitics.

Paper 11088 received Jun. 30, 2011; revised manuscript received Oct. 26, 2011; accepted for publication Nov. 29, 2011; published online Feb. 23, 2012.

1 Introduction

Modern communication systems require superior quality passives for lowpower operation, miniaturization and enhanced performance. With the ability to reconfigure and high-Q as their outstanding properties, radio frequency microelectromechanical systems (RF MEMS) passives are important candidates to achieve these aims. Performance enhancements due to RF MEMS have been demonstrated in design of various circuits like voltage controlled oscillators (VCOs), filters, and matching networks.[1–3]

Next to MEMS switches, MEMS varactors have received considerable attention from industry and academia. Higher tuning ratio and lower-actuation voltage are two of the important design considerations addressed at present. Due to simplicity in design and fabrication, varactors based on electrostatic actuation have been widely studied. Pull-in instability limits the tuning-ratio of parallel plate varactor to 1.5:1. This problem can be overcome by modifying the geometry of the device,[4–7] the series capacitor feedback[8], current drive methods[9] or by closed-loop control. Of the above four methods, only geometry modification does not require adding external components to the varactor. Dual gap varactor[4] leveraged-bending[5] and torsional varactor[6] are the three important designs of geometry modification category. A Dual-gap varactor has been widely fabricated and tested by various groups.[10,11] Recently a linearized MEMS varactor with appropriate post-processing after fabrication through commercial PolyMUMPS process has been presented.[12] The device achieves a dynamic range of 1:5, but requires elaborate postprocessing steps including bulk micromachining of silicon substrate and atomic layer deposition.

We had earlier proposed a torsional MEMS varactor that could outperform other varactor designs.[6,7] The design can be modified to have three-terminal or four-terminal varactor.[6] In this paper we address the effects of parasitics on the performance of three-terminal torsional varactor. Capacitive parasitics are analyzed at low and high frequencies. Parasitics can be mitigated to a great extent using high-resistivity/semi-insulating substrate. However, this is in conflict with typical low-resistivity substrate used for CMOS circuits. In this paper we perform a systematic analysis of parasitic capacitances in torsional varactor fabricated on a low-resistivity substrate (1 to 2Ω cm) and propose an accurate equivalent circuit that emulates the measurement results. Furthermore, the devices are fabricated through PolyMUMPS.[13] Two variants of torsional varactors are proposed to achieve a tuning ratio of capacitance, which is more than 1:8, without any post-processing steps.

1.1 *Design*

Torsional varactor[6] works on the principle of displacement amplification. The structure consists of two sets of parallel plates [Figs. 1(a) and 1(b)]. One of them is used for actuation (DC) and the other is used as the varactor (AC plates). The bottom plates are placed on a substrate. The top actuating plate and top varactor plate are connected to a torsion beam. This arrangement creates a torque on the torsional beam when voltage is applied between the actuating plates. The top varactor plate is placed at a distance sufficiently away from the torsion beam so that it spans the full air-gap smoothly before the actuator plate pulls in. If length L_{2AC} is at least three times the length of, pull-in can be completely avoided in all varactors of this type.

1.2 *Dynamic Range*

The top structure of the torsional varactor moves at an angle to the substrate with applied actuation voltage [Fig. 2(a)]. At a certain voltage the farthest edge (at distance L_{2AC} from the torsion beam) of the top AC plate will touch the bottom plate. This is the maximum downward displacement possible for

0091-3286/2012/$25.00 © 2012 SPIE

the top plate. If the voltage is increased further the top plate will get pressed on the bottom plate [Fig. 2(b)] and capacitance will increase at a different rate. In Fig. 3 the capacitance-voltage curve of a torsional varactor fabricated through the polyMUMPS process is shown. Table 1 gives the dimensions of the device. Figure 3 shows two regions of capacitances. Region 1 corresponds to Fig. 2(a), in which case the top plate moves through the air-gap. Region 2 corresponds to a condition in Fig. 2(b) where the top plate gets pressed on the bottom plate. In region 1, the device

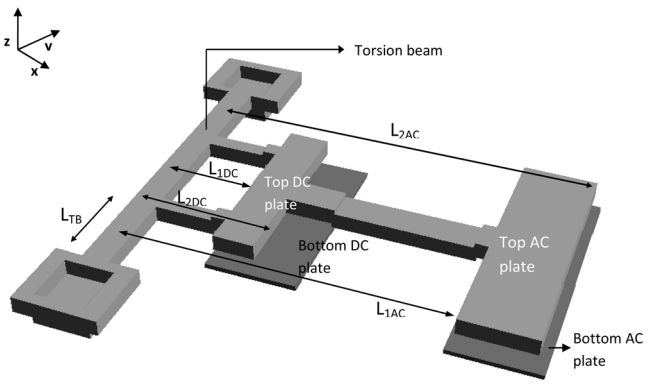

(a)

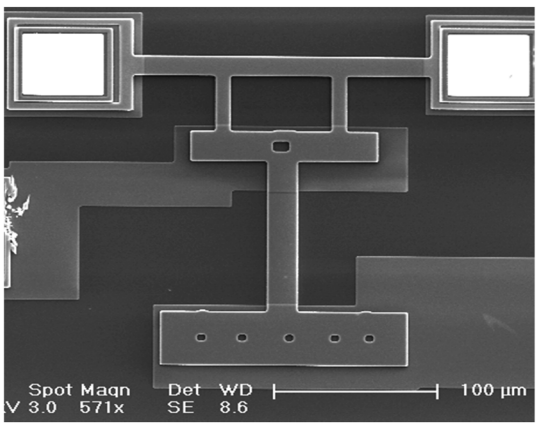

(b)

Fig. 1 (a) Torsional varactor. (b) Scanning electron micrograph (SEM) of torsional varactor.

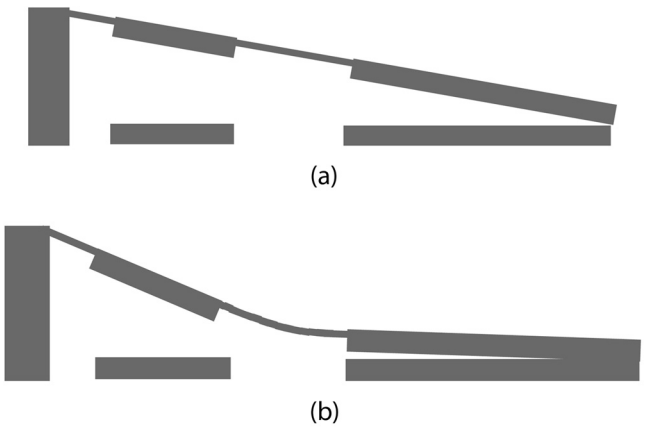

(a)

(b)

Fig. 2 (a) Movement for non-zero actuation voltage (Region 1). (b) Top plate in contact with bottom plate (Region 2).

capacitance increases from 0.035 pF at 0 V to 0.38 pF, offering a dynamic range of 1:10. If the increase of capacitance until 27 V (i.e., region 2) is considered the dynamic range would be 1:16. However, due to reliability considerations,[14] MEMS capacitors are seldom operated in conditions that lead to contact between plates.

In the above analysis, the contribution of parasitic capacitances to the measured capacitances has been excluded. A parasitic capacitance of 0.2 pF was obtained from an identical device without the top structure. This value includes the parasitic capacitances of the bottom varactor plate and probing pads. If the value of parasitic capacitance is added to the values presented in Fig. 3, the tuning ratio would be 1:3. This is one-third of the value obtained without parasitic capacitance making the effect of parasitics on the tuning ratio clearly evident from this analysis. Although the torsional varactor has potential to give high-dynamic range, it suffers from parasitics when fabricated on low-resistivity substrates. In the following sections we characterize the parasitics and propose alternate designs to improve the dynamic range of torsional varactor.

1.3 *Parasitics*

In torsional varactors fabricated through the MUMPS process, the bottom plates are placed on 0.6 μm nitride layer

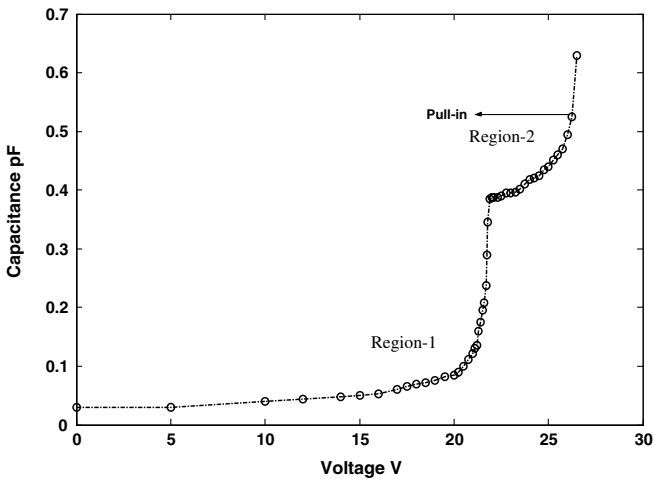

Fig. 3 Measured *C-V* characteristics in two regions of operations.

Table 1 Dimensions of measured varactor.

Length of torsion beam (L_{TB})	55 μm
Width of torsion beam	17 μm
Thickness of torsion beam	2 μm
Gap between top(poly1) and bottom(poly0) plates	2 μm
L_{1DC}, L_{2DC}	55 μm, 80 μm
L_{1AC}, L_{2AC}	200 μm, 245 μm
Area of varactor plate	150×45 μm^2
Area of DC plate	120×25 μm^2

that isolates the plates from the low-resistivity silicon substrate. As shown in Fig. 4, the bottom plate and substrate form two plates of capacitor with nitride as the dielectric layer. Thus, there is a parasitic capacitance associated with plates and pads (used for probing).

For measurements the die with torsional varactor is placed on the chuck of the probe station. The parasitic capacitance measured between a pad of 100×100 μm area and the chuck is 5 pF. This is measured with an inductance, capacitance and resistance (LCR) meter connected across the pad and chuck. The capacitance measured between two pads of similar area placed closely together (50 μm gap) is only 0.2 pF with the chuck connected to ground potential of the measurement system. With the chuck left open the capacitance is 0.3 pF.

When the LCR meter is connected between two pads, the capacitances C_{p1} and C_{p2} are in series. If the substrate behaves as a perfect electrical short between the capacitances, then the resultant capacitance would be 2.5 pF (two 5 pF capacitances in a series). However, in this situation the substrate behaves as a distributed resistor (R_d). This resistor is in series with C_{p1} and C_{p2} and results in reduction in capacitance as seen by the LCR meter. When the chuck is grounded, more signal is lost and hence there is lower measured capacitance between pads. In other words, the connection is equivalent to a series combination of two capacitors and a potentiometer. This model has been verified by connecting discrete components to the LCR meter and varying the resistance.

Figure 5 shows the capacitance-voltage characteristics of a torsional varactor with the chuck grounded and open. There is a difference of nearly 0.1 pF between the capacitance curves at all voltages. The measurements are done at 1 MHz and 20 mV AC excitation signal from the LCR meter. The capacitances measured with grounded chuck were stable, whereas the values with the chuck open were noisy.

Figure 6 shows the *C-V* characteristics of the device at different AC excitation frequencies. The variation in capacitance in all cases is 0.175 pF and the maximum capacitance is reached at the same actuation voltage. However, the capacitance drops with decreasing excitation frequency, due to the fact that the impedance of C_{p1} and C_{p2} increases with a decrease in frequency. Hence the effect of distributed substrate resistance is not as much.

The torsional varactor fabricated with a process similar to polyMUMPS can be modeled with a desired capacitance (C)

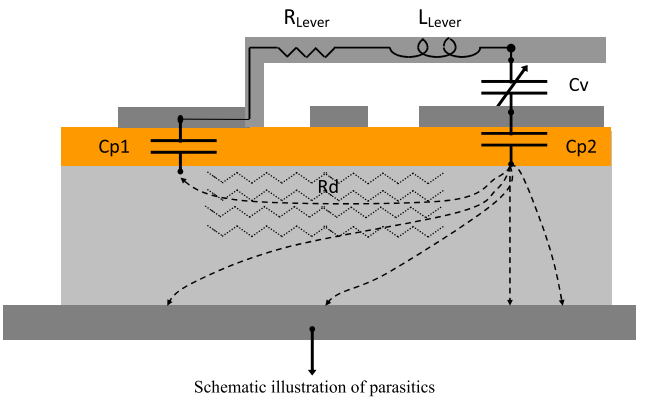

Fig. 4 Schematic illustration of parasitics.

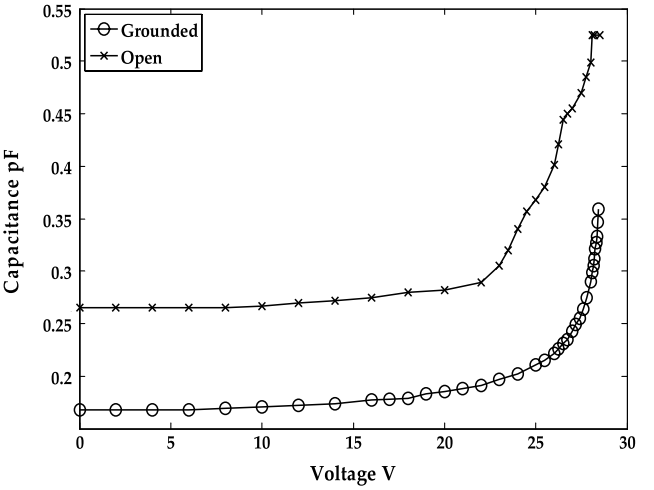

Fig. 5 Measured *C-V* characteristics with grounded and open substrate.

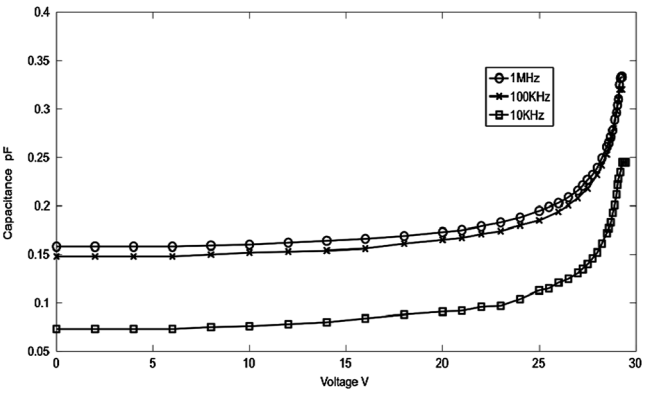

Fig. 6 Measured *C-V* characteristics at different frequencies.

in parallel with parasitic capacitances (C_{p1} and C_{p2} in series). The above analysis shows that as frequency increases, the effects of the substrate become dominant. Refs. 15 and 16 also have presented an analysis of parasitics and residual charge in polyMUMPS process.

1.4 *Parasitics at High Frequencies*

The parasitic capacitances that behave as open circuits tend to become short circuits at high frequencies due to reduced impedance. Measurement results in the previous section showed the impact of parasitic capacitances on the overall capacitance of the device. In this section, we present the analysis of torsional varactor up to 5 GHz, along with the simulated results based on the equivalent circuit for the varactor. As indicated in Fig. 4, the effect of substrate parasitics and a long lever connected to the top plate of the varactor will become important. The effect of lever can be modelled as a series combination of an effective resistance (R_{LEVER}) and an effective inductance (L_{LEVER}).

The test structure used for the high-frequency characterization was a co-panar waveguide (CPW) terminated with torsional varactor as a one-port device. The top structural layer of the torsional varactor is connected to the signal (S) line of transmission and the bottom varactor plate is

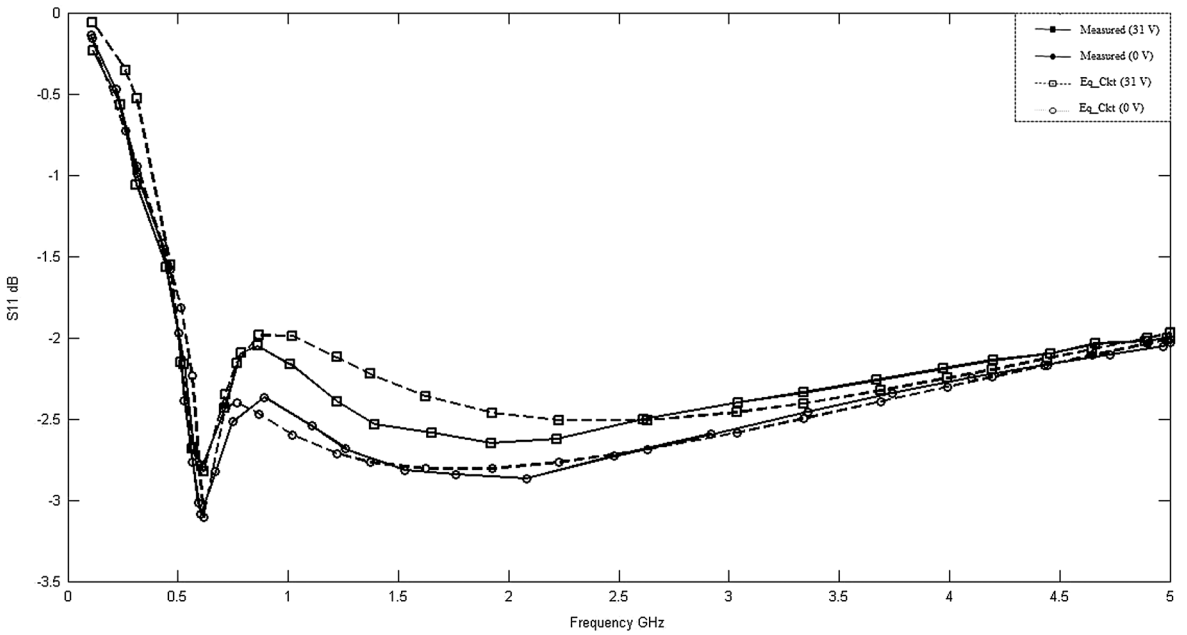

Fig. 7 Measured and simulated reflection coefficient at 0 and 31 V.

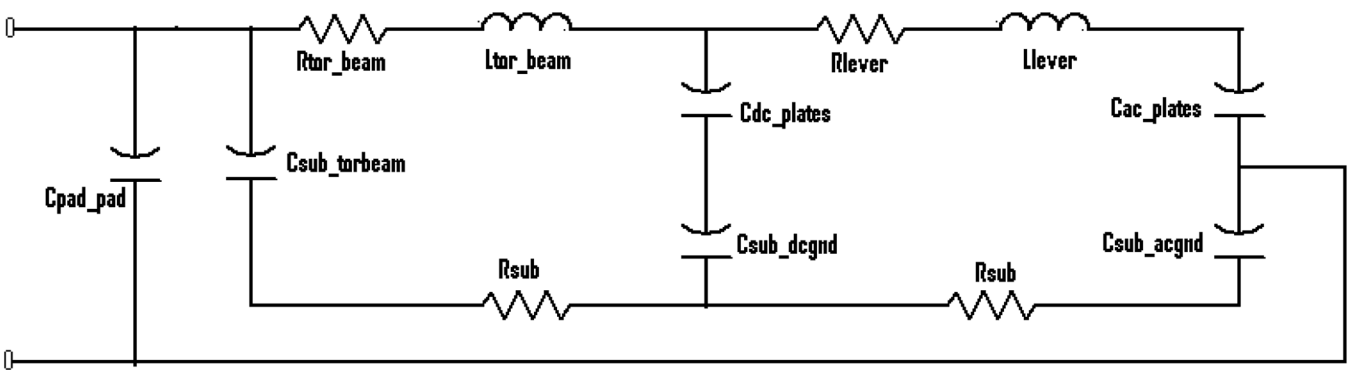

Fig. 8 High frequency equivalent circuit for torsional varactor.

connected to the ground (G) of the transmission line. In Fig. 7, the reflection coefficient ($S11$) of the structure measured at 0 and 31 V is shown, up to the frequency range of 5 GHz. The measurement setup consists of an E8361A PNA network analyzer from Agilent Technologies, a Summit-9000 probe station from Cascade microtech and Infinity probes. Based on the device structure, we developed an elaborate equivalent circuit, as shown in Fig. 8. The torsion beam and levers were modelled with resistors and inductors. AC and DC plates were modelled with capacitance between the plates and parasitic capacitances between the plates and substrate. The substrate is modelled with resistors and simulations were carried out in advanced design system (ADS). The corresponding values of the equivalent circuit element are tabulated in Table 2.

The simulated S parameters for this equivalent circuit are overlaid in Fig. 7 and are shown in dotted lines. We see that the simulated results agree fairly well with the experimental results. Further, it should be noted that the values of the varactor capacitance (Cac_plates) extracted at 0 and 31 V agree fairly well with the low frequency C-V measurements as presented in Fig. 6.

Table 2 Equivalent circuit component values.

Component	Vdc = 0 V	Vdc = 31 V
Cac_plates	0.05 pF	0.3 pF
Cdc_plates	0.015 pF	0.04 pF
Csub_acgnd	1.6 pF	0.72 pF
Csub_dcgnd	0.35 pF	0.35 pF
Csub_torbeam	5.6 pF	5.6 pF
Cpad_pad	0.5 pF	0.5 pF
Rtor_beam	427.5 ohm	300 ohm
Rlever	303 ohm	135 ohm
Rsub	260 ohm	260 ohm
Ltor_beam	37.5 nH	63.5 nH
Llever	1279 nH	180 nH

2 High Dynamic Range Torsional Varactors

2.1 *Bidirectional Varactor*

In the design shown in Fig. 1, the top AC plate moves closer to bottom plate with an increase in actuation voltage, resulting in an increase in capacitance. In some cases where the gap between the plates is low, the dynamic range of capacitance is limited. In order to get a wider dynamic range the design shown in Fig. 9 can be used. MEMS micro-mirrors use a similar structure.

In this design there are two sets of DC actuation plates. The second set of actuation plates (DC2) are attached to torsion beam as shown in the Fig. 9(a). The voltage applied across the DC2 plates moves the AC plate upward, resulting in a decrease in capacitance. The top DC2 plate will move smoothly towards the bottom plate until pull-in happens. Since the AC plate is held farther away from torsion beam, the displacement will be larger than the DC2 plate. Capacitance-Voltage characteristics of two devices with different gaps between AC plates are shown in Fig. 10. The *X*-axis in the figure is partitioned into two regions: AC plate

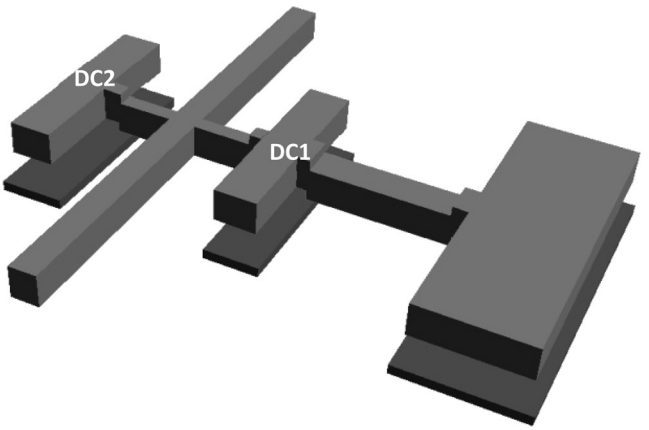

(a)

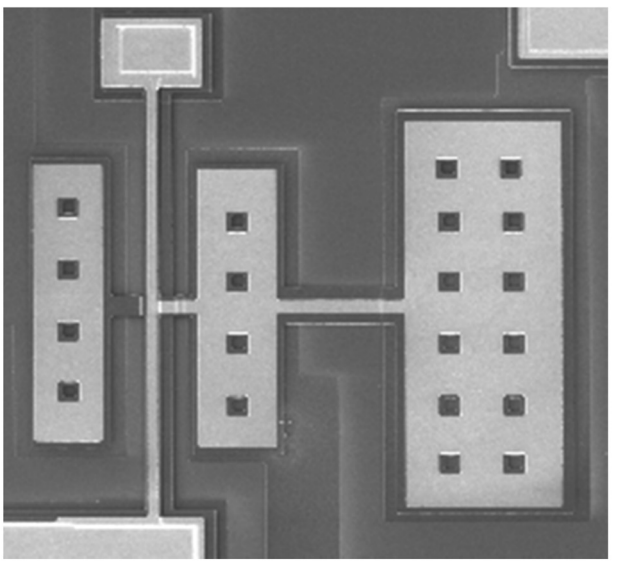

(b)

Fig. 9 (a) Schematic of bidirectional varactor. (b) SEM micrograph of bidirectional varactor (topview).

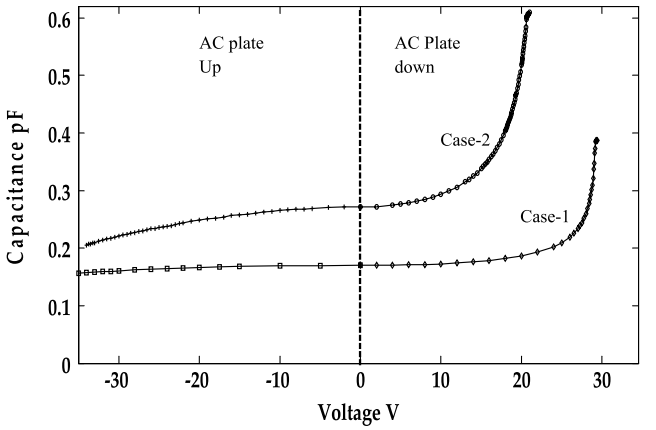

Fig. 10 Measured *C-V* characteristics of varactors with different gaps.

down, indicating the voltage applied on DC1; and AC plate up, indicating the voltage applied on DC2 plate. Two cases are shown in the figure. The gap between AC plates in case1 is 2.75 μm and in case 2 it is 0.75 μm, with the gap between DC plates in both cases being 2.75 μm. Except for the gap between AC plates all other dimensions of the devices are identical.

The top structure is common ground for both DC actuation signal and AC excitation signal. DC actuation voltage is applied to bottom DC plates depending on the direction of movement required. For an increase in capacitance the DC voltage is applied on the bottom plate of DC1 while the bottom plate of DC2 is held at zero. In case 1 the capacitance varies from 0.170 pF at 0 V to 0.38 pF at 29.25 V. When voltage is applied between the DC2 plates the capacitance varies between 0.170 pF at 0 V to 0.153 pF at 37 V. Beyond this voltage pull-in occurs between the DC2 plates. Case 2 shows the *C-V* characteristic of a device with 0.75 μm gap between the AC plates. For actuation voltage applied across DC1 plates the capacitance varied from 0.270 pF at 0 V to 0.610 at 21 V. The capacitance decreased to 0.195 pF at 35.25 V.

The benefit of adding another set of actuation plate can be understood by comparing the improvement in dynamic range obtained in case 1 and case 2. In case 1 the lowest capacitance varies from 0.170 pF to 0.153 pF, resulting in increase in dynamic range from 2.23 (0.380/0.170) to 2.48 (0.380/0.153). In case 2 the increase is from 2.24 (0.610/0.272) to 3.12 (0.610/0.195). Hence, it can be concluded that if the gap between the plates is small the bidirectional torsional varactor can be considered for improving the dynamic range.

2.2 *Suspended Plate Torsional Varactor*

Bidirectional varactor improves the dynamic range by lowering the minimum capacitance possible (C_{min}). But maximum capacitance is same as the unidirectional torsional varactor. It can be seen from Fig. 2(a) that the top plate touches the bottom plate at an angle. More capacitance can be achieved if the plates come in contact over the whole area rather than at the edge. Suspended plate varactor achieves this and extends the maximum capacitance possible (C_{max}). The design requires three conducting layers for fabrication. Furthermore, this design eliminates the effect of substrate

parasitics to a great extent. While the parasitic capacitance due to anchors cannot be avoided, appropriate designs can eliminate the parasitic capacitance due to bottom plates. Suspended plate varactor eliminates the parasitic capacitance due to bottom plate.

Figure 11(a) shows a 3-D view of suspended-plate torsional varactor and Fig. 11(b) shows the side view. The two varactor plates are attached to two separate torsion beams and are being actuated by different actuation signals. The actuation voltage applied on the $DC_{towards}$ pad brings the plates closer and increases the capacitance and voltage applied on DC_{away} reduces the capacitance. This arrangement will require only two actuation signals, one for moving the plates towards each other and another for moving the plates away from each other. If the initial gap between two varactor plates is sufficiently large enough to provide the required dynamic range, then the number of actuation signals can be reduced to just one, to move the plates towards each other alone, for example when only the DC_{toward} signal is required.

A suspended plate varactor with AC plate area of 130×80 μm has been simulated in Coventorware to study the *C-V* characteristics. The gap between the plates is 0.75 μm. The torsion beams and DC plates are optimized to get the maximum dynamic range. Figure 12 shows the *C-V* characteristics. The capacitance is 0.055 pF at 22 V (applied on DC_{away}) and 5 pF at 21 V (applied on $DC_{towards}$), giving a dynamic range of 1:100. The variation of capacitance is smooth with voltage hence it is very promising varactor architecture. The simulation results suggest that for the maximum capacitance of 5 pF, both the suspended plates will move by 0.5 μm, resulting in the minimum distance between the plates

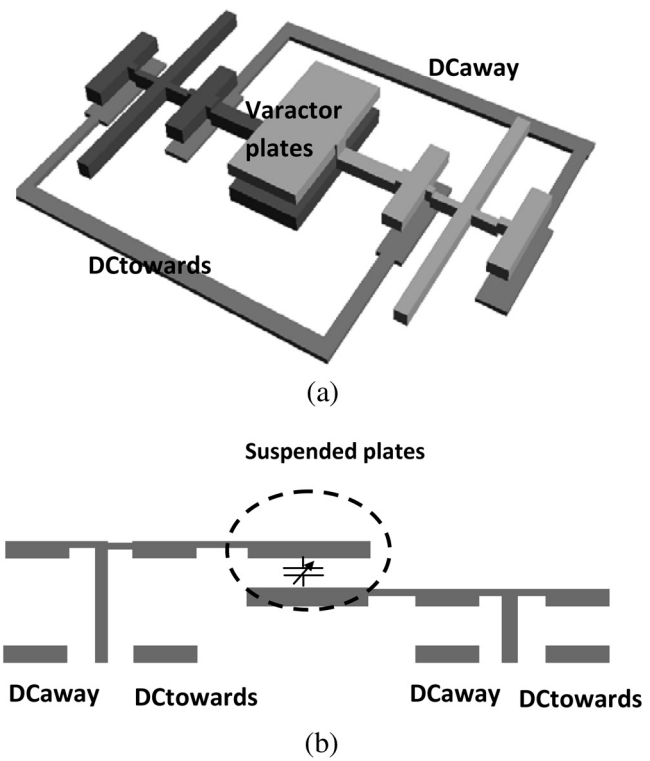

Fig. 11 (a) Suspended-plate torsional varactor. (b) Side-view of suspended-plate varactor.

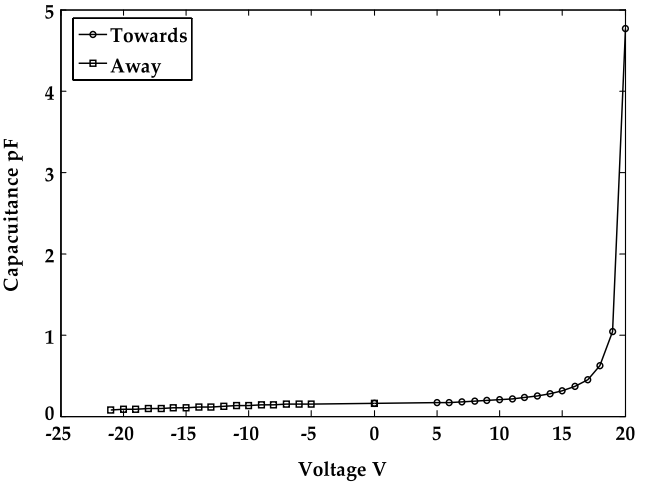

Fig. 12 Simulated *C-V* characteristics of optimized suspended plate varactor.

throughout the plate area. When the plates come closer, the gap between the plates throughout the plate area should be the same [unlike the state in Fig. 2(a), where only the farthest edges of the plates are close]. The dimensions of the plates and beams in the suspended plate varactors must be optimized carefully to achieve this state to get the highest capacitance possible. Another important factor to be considered is residual stress. Residual stress can result in a curvature of the beams,[14] resulting in plates coming into contact at an angle to each other.

Figure 13 shows the SEM micrograph of a suspended-plate torsional varactor fabricated through polyMUMPS. The bottom DC plates are made of poly0, with the bottom AC plate made of poly1 and the top AC plate made of poly2. This offers a gap of 0.75 μm between the AC plates. The *C-V* characteristic of a floating plate suspended varactor is shown in Fig. 14. The device had an AC plate area of 130×80 μm. When the plates are moved towards each other with actuation voltage applied on $DC_{towards}$ plates, the capacitance varies from 0.14 to 0.35 pF. The dynamic range is 2.5. When

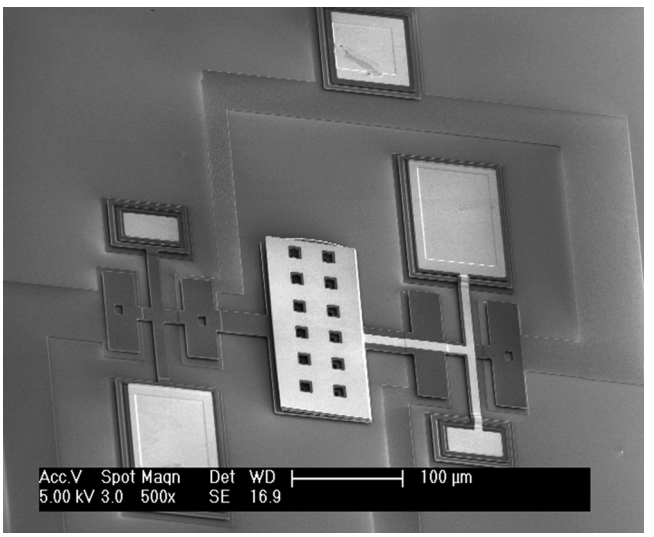

Fig. 13 SEM micrograph of suspended-plate varactor.

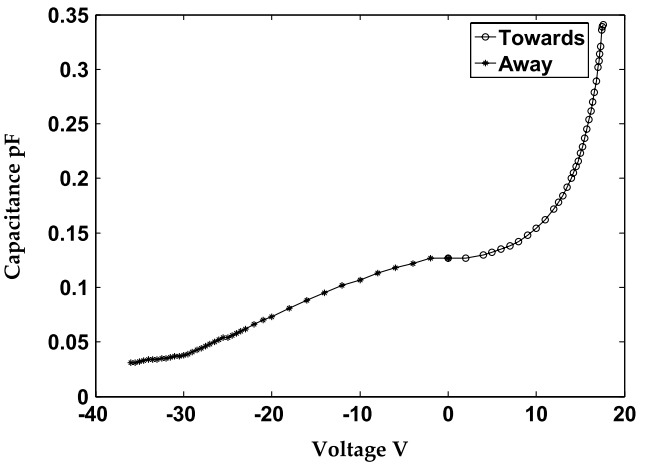

Fig. 14 Measured *C-V* characteristics of suspended varactor.

the actuation voltage is applied across DC_{away} plates the capacitance varies from 0.14 pF to 0.045 pF. If this minimum capacitance is taken into account for calculating the dynamic range, we get a tuning-ratio of more than 1:8. It should be noted that the measured capacitance shown in Fig. 14 includes the parasitic capacitances due to anchors and pads and the parasitics are not subtracted, as in the earlier cases.

The dymanic range of 1:8 exhibited by the device fabricated through polyMUMPS is much lower than the simulated results thatshowed a dynamic range of 1:100. In the MUMPS device discussed above, the thicknesses of the beams are different and the plate dimensions are not optimized for maximum capacitance state. So the plates would have come into contact only at the edges.

Some of the devices were taken beyond the point of contact by increasing the applied voltage. When the actuation voltage is increased further the plates would be pressed against each other so that larger areas of the plates come into contact, resulting in a further increase in capacitance. The capacitance increased smoothly from 0.22 pF at 0 V to 0.625 pF at 17.8 V, then increased sharply at 18.1 V to 0.836 pF. From 0.836 pF the increase was smooth until 1.2 pF, when the value jumped to 1.75 pF at 22.5 V.

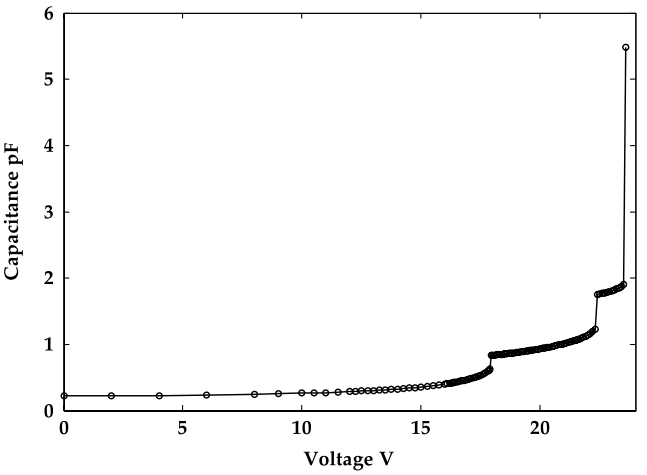

Fig. 15 Extended *C-V* characteristics of suspended varactor at higher voltages until failure.

Then the increase was smooth until 1.91 pF. Between each increment in voltage the actuation voltage was removed to check whether the device reverts back to its zero-voltage-capacitance. Until 1.91 pF, at 23.5 V the device was working fine. At 23.7 V the device failed permanently and the capacitance did not revert back to 0.22 pF after actuation voltage was removed. The capacitance at this voltage shot up to 5.5 pF, as shown in Fig. 15.

These results show that suspended plate varactors can offer a very high dynamic range but the devices need to be optimized carefully so that the plates come in contact throughout the area during the point of contact. A simple way is to choose the gap between the DC plates, the area of DC plates, the length, width and thickness of the torsion beams and the length of the lever on both sides equal. This would ensure that both plates undergo the same rotation and displacement. Hence the whole area of AC plates will be in contact with each other when maximum capacitance is reached. However, residual stress can result in the bending of beams and plates and a change of gap between plates.[14,16,17] As both plates are suspended in suspended-plate varactor more attention needs to be given to residual stress in the design stage.

3 Conclusions

This work presents the analysis of parasitics associated with torsional varactors at low and high frequencies. The simulation results on the equivalent circuit are validated against the measured experimental results. The effect of the parasitics on the tuning ratio was emphasized and designs to improve the tuning ratio were presented. The bidirectional varactor presented can be fabricated through a two-layered fabrication process. The suspended-plate varactor requires a three-layer process, and the one realized through PolyMUMPS process yielded a dynamic range of 1:8 by eliminating the effect of parasitic capacitances. It was also shown through the simulations that suspended plate varactors could attain a dynamic range of up to 1:100, if optimized properly.

References

1. G. M. Rebeiz, *Rf MEMS Theory, Design and Technology*, Wiley-Interscience, New Jersey (2003).
2. H. J. D. L. Santos, *RF MEMS Circuit Design for Wireless Applications*, Artech House, Boston (2002).
3. H. J. De et al., "RF MEMS for ubiquitous wireless connectivity Part 2-application," *IEEE Microwave Mag.* **5**(4)50–65 (2004).
4. J. Zou et al., "Development of a wide tuning range MEMS tunable capacitor for wireless communications systems," in *IEEE International Electron Devices Meeting (IEDM '00) Technical Digest*, San Francisco, CA, USA, pp. 403–406 (2000).
5. E. S. Hung and S. D. Senturia, "Extending the travel range of analog-tuned electrostatic actuators," *J. Microelectromech. Syst.* **8**(4), 497–505 (1999).
6. C. Venkatesh, P. Shashidhar, and B. Navakanta, "Torsional MEMS varactor with low actuation voltage," Special Issue on Microelectromechanical Systems, *Int. Comput. J. Eng. Sci.* **4**, 555–558 (2003).
7. C. Venkatesh et al., "A torsional MEMS varactor with wide dynamic range and low actuation voltage," *Sens. Actuators A* **121**, 480–487 (2005).
8. J. I. Seegar and S. B. Crary, "Stabilization of electrostatic actuated mechanical devices," in *Proc. Transducers'97*, Chicago, IL, USA, pp. 1133–1136 (1997).
9. L. Castaner et al., "Analysis of the extended operation range of electrostatic actuators by current-pulse drive," *Sens. Actuators A* **90**(3), 181–190 (2001).
10. G. S. M. Rijks et al., "RF MEMS tunable capacitors with large tuning ratio," in *Digest of Technical Papers, IEEE MEMS-2004*, pp. 777–780 (2004).
11. T. K. K. Tsang and M. N. El-Gamal, "Very wide tuning range micro-electromechanical capacitors in MUMPS process for RF applications,"

Digest of Technical Papers, Symposium on VLSI circuits, pp. 33–36 (2003).
12. M. Bakri-Kassem and R. R. Mansour, "Linear bilayer ALD coated MEMS varactor with high tuning capacitance ratio," *J. Microelectromech. Syst.* **18**(1), 147–153 (2009).
13. D.A. Koester et al., "MUMPS Design Handbook," Revision 5.0, Cronos Integrated Microsystems, Research Triangle Park, NC (2000).
14. C. Venkatesh and N. Bhat, "Reliability analysis of torsional MEMS varactor," *IEEE Trans. Device Mater. Reliab.* **8**(1), 129–134 (2008).
15. E. K. Chan and R. W. Dutton, "Effects of capacitors, resistors and residual charge on the static and dynamic performance of electrostatically actuated devices," *Proc. SPIE* **3680**, 120–130 (1999).
16. A. M. Elshurafa and E. I. El-Masry, "Design considerations in MEMS parallel plate variable capacitors," in *Proc. MWSCAS-2007*, Montreal, Quebec, pp. 1173–1176 (Aug 2007).
17. A. Dec and K. Suyama, "Micromachined electro-mechanically tunable capacitors and their applications to RF ICs," *IEEE Trans. Microwave Theor. Tech.* **46**(12), 2587–2596 (1998).

Chenniappan Venkatesh received his BE in instrumentation and control from the National Institute of Technology, Trichy in 1998, MSc (engineering) from the Indian Institute of Science in 2001 and PhD from Indian Institute of Science in 2008. From 2008 to 2010 he was with the University of Newcastle, Australia as a post-doctoral fellow. At present he is at the University of Western Australia as post-doctoral researcher. His research interests include MEMS, systems dynamics and control and photonics.

Navakanta Bhat received his BE in electronics and communication from the University of Mysore in 1989, MTech in microelectronics from I.I.T. Bombay in 1992 and PhD in electrical engineering from Stanford University, Stanford, CA in 1996. Then he worked at Motorola's Networking and Computing Systems Group in Austin, TX until 1999. At Motorola he worked on logic technology development, and he was responsible for developing high-performance transistor design and dual gate oxide technology. He joined the Indian Institute of Science, Bangalore in 1999 where he is currently a professor in the Centre for Nano Science and Engineering and Electrical Communication Engineering department. His current research is focused Nano-CMOS technology and Integrated CMOS-MEMS sensors. The work spans the domains of process technology, device design, circuit design and modeling. He has 150 research publications in international journals and conferences and five U.S. patents.

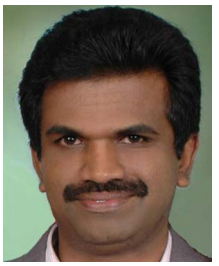

K. J. Vinoy is an associate professor in the Department of Electrical Communication Engineering at the Indian Institute of Science (IISc), Bangalore, since 2003. He received BTech from the University of Kerala, MTech from Cochin University of Science and Technology, India, and PhD from the Pennsylvania State University, USA, in 1990, 1993, and 2002, respectively. From 1994 to 1998 he worked at National Aerospace Laboratories, Bangalore, India. From 1999 to 2002, he worked as a research assistant and from 2002 to August 2003 as a Postdoctoral fellow at the Pennsylvania State University. His research interests include several aspects of microwave engineering such as fractal antennas, wideband antennas, passive circuits, RF-MEMS and Computational Electromagnetics. He has published over 130 papers and four books. He has one US Patent awarded and three Indian patents filed. He is in the editorial boards of three journals. He is a fellow of the Indian National Academy of Engineering.

Satish Grandhi received his BE in electronics and communication engineering (ECE) from Andhra University, Vishakapatnam, India in 2005 and his MTech in microelectronics from NITK Surathkal, Mangalore, India in 2007. He is currently working as a senior electrical design engineer with Cypress Semiconductor, Bangalore, India.